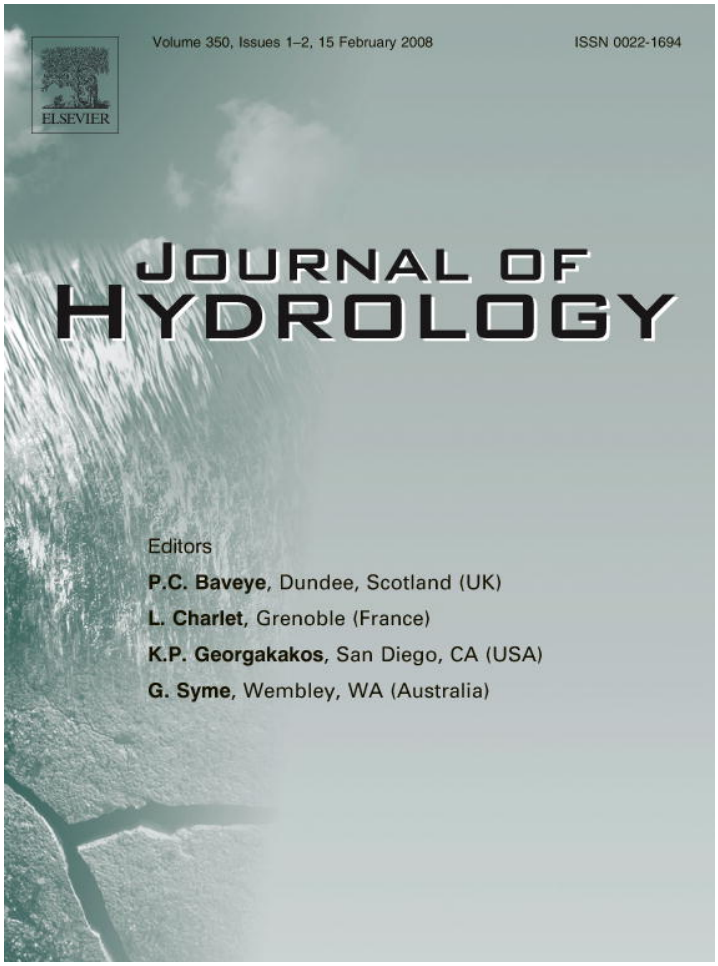

Journal of Hydrology (2008) **350**, 25–40

available at www.sciencedirect.com

ScienceDirect

journal homepage: www.elsevier.com/locate/jhydrol

Hydrochemical variations and contaminant load in the Río Tinto (Spain) during flood events

C.R. Cánovas [a,*], C.G. Hubbard [b], M. Olías [a], J.M. Nieto [c], S. Black [b], M.L. Coleman [b,d]

[a] *Department of Geodynamics and Palaeontology, University of Huelva, Campus el Carmen, 21071 Huelva, Spain*
[b] *School of Human and Environmental Sciences, University of Reading, Reading, Berks RG6 6AB, United Kingdom*
[c] *Department of Geology, University of Huelva, Campus el Carmen, 21007 Huelva, Spain*
[d] *CALTECH, Jet Propulsion Laboratory, 4800 Oak Grove Dr, Pasadena, CA 91109, USA*

Received 19 March 2007; received in revised form 15 November 2007; accepted 19 November 2007

KEYWORDS
AMD;
Río Tinto;
Metal load;
Flood events

Summary The aim of this work is to study the hydrochemical variations during flood events in the Río Tinto, SW Spain. Three separate rainfall/flood events were monitored in October 2004 following the dry season. In general, concentrations markedly increased following the first event (Fe from 99 to 1130 mg/L; Q_{max} = 0.78 m^3/s) while dissolved loads peaked in the second event (Fe = 7.5 kg/s, Cu = 0.83 kg/s, Zn = 0.82 kg/s; Q_{max} = 77 m^3/s) and discharge in the third event (Q_{max} = 127 m^3/s). This pattern reflects a progressive depletion of metals and sulphate stored in the dry summer as soluble evaporitic salt minerals and concentrated pore fluids, with dilution by freshwater becoming increasingly dominant as the month progressed. Variations in relative concentrations were attributed to oxyhydroxysulphate Fe precipitation, to relative changes in the sources of acid mine drainage (e.g. salt minerals, mine tunnels, spoil heaps etc.) and to differences in the rainfall distributions along the catchment. The contaminant load carried by the river during October 2004 was enormous, totalling some 770 t of Fe, 420 t of Al, 100 t of Cu, 100 t of Zn and 71 t of Mn. This represents the largest recorded example of this flush-out process in an acid mine drainage setting. Approximately 1000 times more water and 140–8200 times more dissolved elements were carried by the river during October 2004 than during the dry, low-flow conditions of September 2004, highlighting the key role of flood events in the annual pollutant transport budget of semi-arid and arid systems and the need to monitor these events in detail in order to accurately quantify pollutant transport.

* Corresponding author. Address: Facultad Ciencias Experimentales. Campus el Carmen, s/n, 21007, Spain. Tel.: +34 959219870; fax: +34 959219440.
E-mail address: carlos.ruiz@dgeo.uhu.es (C.R. Cánovas).

0022-1694/$ - see front matter
doi:10.1016/j.jhydrol.2007.11.022

Introduction

Acid mine drainage (AMD) is one of the main causes of water pollution worldwide. This water polluting process is mainly related to mining of massive sulphide and coal deposits. Sulphides are stable and very insoluble under reducing conditions, but oxidation takes place when minerals are exposed to atmospheric conditions. Release of acidity, sulphates, iron and accessory metals and metalloids (e.g. Cu, Zn, Co, Cd, Ni, As, etc.) from the oxidation of sulphides affects the quality of streams and groundwaters. A detailed description of reactions controlling sulphide oxidation can be found in Nordstrom and Alpers (1999).

The headwaters of the Río Tinto in the SW of Spain (Fig. 1) are situated in the Iberian Pyrite Belt (IPB), which hosts one of the largest concentrations of massive sulphide deposits in the world (Tornos, 2006). The river has attracted a wide range of studies: archaeological investigations (e.g. Nocete et al., 2005) combined with sediment cores from the estuary and continental shelf (Leblanc et al., 2000; Ruiz et al., 1998; van Geen et al., 1997) have shown that the Riotinto mining district has been exploited for at least 4500 years, while the presence of an Fe based ecosystem of extremophile bacteria (González-Toril et al., 2003a; López-Archilla et al., 2001, 2004) and eukaryotes (Zettler et al., 2002) have garnered interest in the river as a potential natural analogue system for hydrometallurgical processes (González-Toril et al., 2003b; Malki et al., 2006) and extraterrestrial systems (Fernández-Remolar et al., 2003, 2004, 2005).

Amongst the rivers affected by AMD worldwide, Río Tinto is an extreme case of pollution with low pH values (between 1.0 and 3.0) and very high metal and metalloid concentrations along its main course (100 km long). Table 1 shows average concentrations and annual loads of metals and metalloids in several rivers. Río Tinto is extremely polluted,

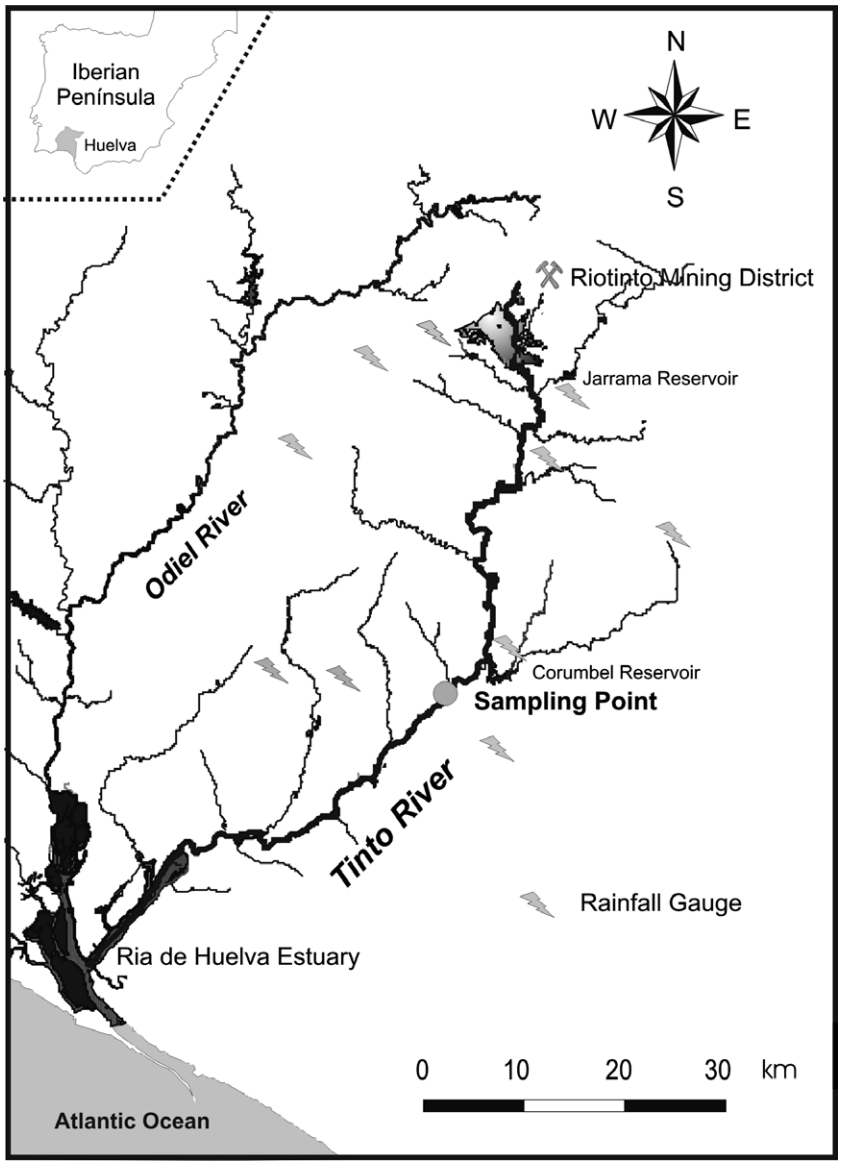

Figure 1 Map of the Río Tinto showing the location of the sampling point, the mining area and the pluviometric gauges.

showing values of metal concentration notably larger than the rest of the rivers. Furthermore, in spite of having a drainage basin appreciably smaller, metal loads transported by Río Tinto are in some cases (Cd, and Cu) larger than the metal loads transported by rivers such as Rhone, Elbe and Seine, which drain some of the most industrialised regions in Europe.

The identification of anomalously high trace metal concentrations in the Western Mediterranean Sea and the Gulf of Cadiz (Boyle et al., 1985; van Geen et al., 1991) resulted in a major EU funded project entitled TOROS (Tinto Odiel River Ocean System), which examined the metal biogeochemistry of the Río Tinto and adjacent Río Odiel rivers (Fig. 1), their mixing zones and the Gulf of Cadiz (Achterberg et al., 2003; Braungardt et al., 2003; Elbaz-Poulichet et al., 2001). The importance of the Tinto and Odiel rivers as metal sources for the Western Mediterranean Sea has led to a number of estimates of the dissolved metal loads transported by these rivers (Braungardt et al., 2003; Olías et al., 2006; Sainz et al., 2004; Sarmiento et al., 2004).

Rivers in mediterranean climate regions, such as Río Tinto, alternate long drought periods and short but intense rainfall events during which most of the water discharge, dissolved contaminant, and suspended matter transport occurs. Sainz et al. (2004) stated that flood events (discharge > 10 m^3/s) occured on average 17% of the time but delivered over 50% of the annual dissolved metal load. Flood events are therefore, key to understanding metal transport processes in this mediterranean catchment. These examples of mass flow are scarcely documented and hence, largely unknown as previous studies estimating dissolved loads have only sampled the river on a weekly basis (at best) and therefore have failed to accurately capture these key events.

The aims of this work therefore are: (1) to study the hydrogeochemical changes in a highly polluted river such as Río Tinto during storm events; (2) to estimate the mass fluxes that take place during these events and (3) to quantify the importance of flood events in the annual metal loads into the Ría de Huelva estuary.

Site description

The source of the Río Tinto is commonly accepted to be in the abandoned mining area of Peña del Hierro (Ferris et al., 2004), some 450 m above sea level. From here the river runs through the Riotinto mining district before flowing down to the Atlantic coast of Spain by the city of Huelva (Fig. 1). The river is approximately 100 km long and drains a catchment with a surface area of 1646 km^2. The Jarrama and Corumbel rivers are its main tributaries (Fig. 1), although they are regulated by reservoirs before their confluences with the Río Tinto.

The upper and middle parts of the catchment are underlain by paleozoic rocks belonging to the Iberian Pyrite Belt (IPB), which comprises of the Phillite-Quartzite (PQ) group overlain by the Volcano-Sedimentary Complex (VSC, formed by slates, shales, volcanic and volcaniclastic rocks) and the Culm group (formed by shales and greywakes). The lower part of the catchment is underlain by Neogene detrital materials (sands, silts, clays, etc.), belonging to the Guadalquivir Basin.

The climate is of a dry mediterranean type with an average rainfall varying between 600 mm in the lower part of the catchment and 1000 mm in the upper northern hills. The rainfall distribution displays great inter- and intra-annual variations, with 70% of the annual rainfall occurring between October and February, while rainfall is almost non-existent during the dry season from June to September.

Table 1 Element concentrations and loads transported by rivers worldwide

River	Catchment km^2	Discharge m^3/s	Al	As	Cd	Cu	Fe	Mn	Pb	Zn
			Dissolved concentrations (mg/L)							
Río Tinto[a]	1646	1.6	75	0.86	0.25	27.2	393	11.4	0.19	61.8
Thames[b]	12,935	65.8		0.003		0.004		0.1	<0.001	
Seine[c]	78,650	435		0.001	0.03	0.002		0.006	<0.001	
Rhone[d]	159,127	2170		0.002	0.03	0.002			<0.001	
Mississippi[e]	2981,000	12,743			<0.001	0.02				0.003
Amazon[d]	7050,000	219,000			0.06	0.02				<0.004
Streams average[f]			0.05	0.002		0.007	0.04	0.008	0.001	0.03
			Annual load (ton/yr)							
Río Tinto[a]	1646	1.6	1234	12.4	3.9	469	5075	163	14.8	863
Seine[g]	78,650	435			0.44	25			9	135
Elbe[h]	131,950	720		16.3	2.5	51.4			22.8	501
Rhone[h]	159,127	2170		40.4	2.5	149.5			225.9	966

[a] Olías et al. (2006).
[b] Neal et al. (2000).
[c] Elbaz-Poulichet et al. (2006).
[d] Boyle et al. (1982).
[e] Stumm and Morgan (1996).
[f] Drever (1997).
[g] Thevenot et al. (2007).
[h] Vink et al. (1999).

The Río Tinto catchment is mainly underlain by low permeability materials and consequently river discharge is highly dependent on the rainfall regime. Olías et al. (2006) showed that during the 1995–2003 period, the Río Tinto's annual average discharge was 50 h m^3, with a minimum value of 6 h m^3 and a maximum of 79 h m^3. River discharge was low (<1 m^3/s) for 78% of the recorded days, only exceeding 10 m^3/s in 4% of the days, coinciding with flood events.

The headwaters of the Río Tinto drain the historic mining districts of Peña del Hierro and Riotinto. The Riotinto Mining District is formed by several polymetallic massive sulphide deposits which can be classified in two groups according to their geographical location. Group North is formed by Lago, Dehesa and Salomon deposits, while Group South is constituted by Filon Sur and the big sulphide deposit of San Dionisio. As a consequence of mining activities developed in the area since ancient times, numerous point inputs enter the river from a variety of waste piles associated with mining activities (gangue materials from ore extraction, smelting residues, settling ponds and waste from heap leaching), together with tunnels draining underground workings.

Three main AMD inputs could be differentiated (Hubbard, 2007). At its source, Río Tinto receives leachates from the old mine of Peña de Hierro with a low pH (1.6) and extremely elevated concentrations of sulphate (81 g/L), metal and metalloids (22,700 mg/L of Fe, 4600 mg/L of Al, 13 mg/L of As, 27.4 mg/L of Co, etc.) although their most striking characteristic is the low concentration of Cu and Zn (20 mg/L of Cu and 21 mg/L of Zn). Discharges coming from tunnels draining underground workings in the Ríotinto Mining District, such as Tunnel 11 and Tunnel 16 (4.5 and 7.2 km downstream from source, respectively), have higher values of pH (2.7–3.0), Cu and Zn (up to 463 and 528 mg/L, respectively) but lower values of sulphates (up to 18,360 mg/L), Fe (up to 3050 mg/L), Al (up to 1330 mg/L), etc. Drainages coming from the Zarandas-Naya mine (8.3 km downstream from the source) join the Rio Tinto waters through the Arroyo Alcojola, which has extremely low pH values (1.2–1.5) and transports large amounts of sulphate (55.5 g/L), metals and metalloids (22,100 mg/L of Fe, 1620 mg/L of Al, 538 mg/L of Cu, 540 mg/L of Zn, 99 mg/L of Mn, 88 mg/L of As, etc.).

The chemical composition of these drainages varies throughout the year owing mainly to hydrologic (i.e. rise of water table, differences in hydraulic behaviour in tailing piles, slag heaps, settling ponds, etc.) biological (bacterial activity) and anthropogenic factors (pumping from mine sites, etc.), recording the highest sulphate and metal concentrations during the summer, when the biotic oxidation processes are more intense, and the lowest during the winter, when dilution by infiltration water takes place.

The resultant AMD decreases in concentrations and increases in pH as it travels downstream due to dilution from freshwater tributaries (such as the Jarrama and Corumbel rivers) and sorption to/coprecipitation with Fe oxyhydroxides and oxyhydroxysulphates (Galán et al., 2003; Hudson-Edwards et al., 1999).

Despite dilution and sorption/precipitation processes, the river still maintains high concentrations of pollutants before it enters the estuary, with a mean pH of 2.8 (range 2.2–5.0), electrical conductivity of 2.5 m S/cm (range 0.43–9.0 m S/cm) and dissolved metal concentrations of 151 mg/L of Fe (range 0.07–2804 mg/L), 18.9 mg/L of Cu (range 0.2–134 mg/L), 26.0 mg/L of Zn (range 2.2–152 mg/L) measured at Niebla, approximately 61 km downstream of the river source (Cánovas et al., 2007).

Acidity decreases in the estuary as seawater mixes with river water, although metal removal processes are inefficient until high salinities are reached (e.g. Achterberg et al., 2003; Braungardt et al., 2003; Elbaz-Poulichet et al., 1999; López-González et al., 2006). Metal removal processes result in the metallic enrichment of estuarine sediments, with the mobility and bioavailability of metals such as Zn, Cd and Cu being higher in sediments located in the area of fresh water influence than in sediments located in the marine influenced area of the estuary (Nieto et al., 2007).

Methodology

The sampling site was located at a stream-gauge station at Gadea, approximately 41 km downstream of the Riotinto mining area and 50 km downstream of the river's source. Rainfall data have been obtained from pluviometric gauges spread over the catchment (Fig. 1).

Sampling was performed by a Xian 1000 portable autosampler from Bühler Montec. The autosampler consisted of a sample container holding up to 24 bottles and an outlet pipe made of polyethylene. Bottles were washed in 10% (v/v) nitric acid and then with milli-Q water (18.2 MΩ) prior to sampling. Samples were pumped by an air pump vacuum system and manual samples were taken when the autosampler did not work. Before taking a sample, the equipment was automatically purged with river water to avoid sample cross-contamination. The frequency of the sampling was every two, three or six hours depending on the forecast, and being more frequent during flood events (2 h). Electrical conductivity (EC), pH, redox potential (Eh) and temperature were measured in situ for all samples using portable meters HI-9025C and HI-9033. Samples were filtered through 0.45 μm teflon filters, acidified with suprapure nitric acid to a pH <2 and refrigerated until analysis.

Twenty-five samples were selected for analysis from all those taken in October 2004. Samples were selected when significant changes in pH and EC were observed. The chemical analysis was undertaken at the Central Research Services of the University of Huelva following a custom-designed protocol specific to these types of water (Ruiz et al., 2003). A wide range of major elements (Al, Ca, Cu, Fe, K, Mg, Mn, Na, S, Si and Zn) and trace elements (As, Ba, Be, Cd, Co, Cr, Li, Mo, Ni, P, Pb, Sn and Sr) were analysed using Inductively Coupled Plasma Optical Emission Spectroscopy (ICP-OES) on a Jobin Yvon (JY ULTIMA 2) spectrometer. A triplicate analysis was performed in order to evaluate the analytical precision, showing differences below 5% in all cases. Detection limits (3σ of analytical blanks) were below 0.14 mg/L for major elements and 7.04 μg/L for trace elements. The analytical accuracy was checked by the analysis of reference materials (SPS-SW2, TMDA-54.3 and NIST-1640) and an interlab comparison with the University of Reading (Perkin Elmer

Optima 3000 ICP-OES and Elan 6000 ICP-MS), using samples from across the EC range. Most of the elements assessed in the interlab comparison showed differences below 5%.

Fifteen salt mineral samples were collected in August 2003 and September 2004 and analysed at the University of Reading by XRD with a Bruker D5000 using Diffrac AT software and by XRF with a Philips PW1480 Sequential Spectrometer and (for As) a portable Niton XLt 700 XRF Analyser.

Results and discussion

Rainfall and discharge variations

Fig. 2 shows the hydrograph during the study period as well as the daily average rainfall recorded in the catchment and the samples analysed for dissolved concentrations. The lack of rainfall during the dry season (June—September) caused the river discharge to decrease from 0.24 m^3/s in June to 0.004 m^3/s at the beginning of October. A comparison of total discharge highlights the extreme seasonality of the Río Tinto with 10.4 hm^3 of water recorded at Gadea in October 2004, compared with a total discharge of 0.01 hm^3 in September. Three different flood events have been identified from the hydrograph.

The river discharge increased from 0.004 to 0.78 m^3/s due to the first rainfall (on the 8th and 9th of October) recorded after a long dry season. This maximum was reached 10 h after the end of the rainfall. The lag between the rainfall and the hydrograph crest can be explained by the basin concentration time and the low moisture content in the catchment soils after the dry season (Walling and Foster, 1975). After this peak, the discharge decreased gradually to 0.12 m^3/s. Unfortunately, the autosampler did not work during this event so its impact on the river could only be assessed by comparing pre-event and post-event samples from the 2nd and 18th of October.

The second rainfall event (Event 2) occurred from the 18th to the 21st of October and can be divided into three sub-events with discharge peaks of 0.87 m^3/s (Event 2a), 6.4 m^3/s (Event 2b) and 77 m^3/s (Event 2c). The rising limb of Event 2c was not sampled because sediments mobilised by rapidly rising water levels buried the inlet pipe of the autosampler, although some samples were taken manually during the falling limb. The third and final flood event of October 2004 occurred on the 27th as a consequence of an average rainfall in the catchment of around 80 mm. This event had the highest peak discharge (127 m^3/s) recorded in the month. The falling limb appeared to be stepped (Fig. 2), which can be explained by the water released into the Río Tinto from the Jarrama reservoir (Fig. 1) on the 28th (2.2 hm^3) and the 29th (1.4 hm^3).

Hydrogeochemical variations

In order to analyse the hydrogeochemical changes during storm events that occur after a long dry season in a complex system like Río Tinto, it is necessary to consider all the processes and sources that might affect the water composition: (1) washout of soluble efflorescent salts precipitated during the summer; (2) dilution by runoff freshwater; (3) spatial variations of rainfalls between undisturbed and mining areas; (4) precipitation of iron mineral phases; and (5) variations in contribution from different AMD inputs.

Basic statistics from samples collected during the storm events are shown in Table 2. Fig. 3 shows variations in pH, EC and some dissolved compounds throughout the flood events. Sulphate concentrations increased dramatically following Event 1 from 1.6 g/L on 02/10/04 to 9.5 g/L on 18/10/04 reaching an apparent steady state of elevated concentrations. This could be caused by the dissolution of soluble evaporitic salt minerals accumulated on the banks of the Río Tinto and on/in spoil heaps in the Source Zone (Buckby et al., 2003; Lottermoser, 2005) or by water richer in sulphate emanating from other AMD sources.

During this first event, most elements raised their concentration, being As the element which showed the maximum increase (nearly 2 orders of magnitude). However some elements such as Na, Sr and K underwent a slight decrease.

Concentrations remained high through Event 2a with some elements increasing (e.g. Fe, As and Pb) while others remained constant (e.g. Al, Co, Mn, Ni, Zn), despite the increase in discharge. The slow dissolution of less soluble mineral phases owing to the acidity released by dissolving

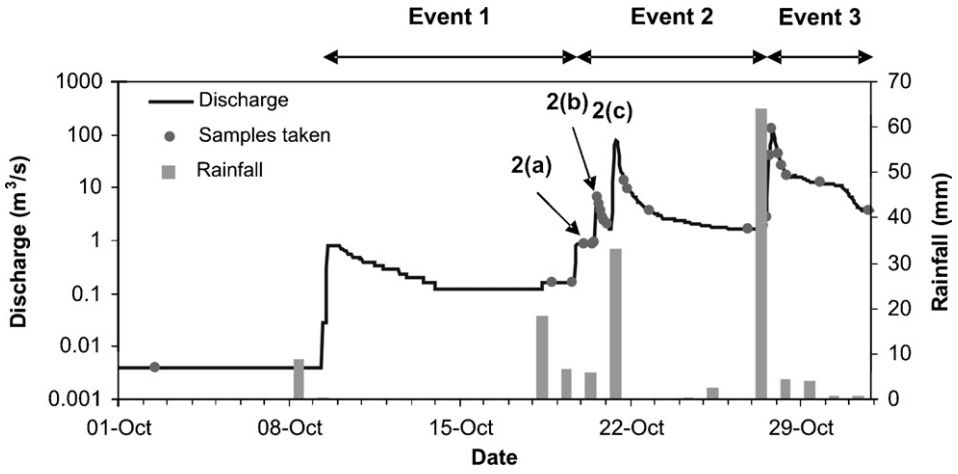

Figure 2 Rainfall and discharge data for the monitored period.

the evaporitic salt minerals, could explain this increase. Pb and mainly As, have a great affinity to be adsorbed onto Fe mineral phases (e.g. Zänker et al., 2002; Acero et al., 2006).

Concentrations then decreased steadily through Event 2b although Pb (Fig. 3), and Ba exhibited a different behaviour. The crest of the hydrograph for Event 2b did not occur at the same time as the minimum value of EC and sulphate and metal concentrations (Fig. 3). Variations in concentration of dissolved elements usually show a lag with water discharge (Lee and Bang, 2000; Sandén et al., 1997; Walling and Foster, 1975), which is inversely related to antecedent catchment soil moisture and rainfall magnitude. No such lag was apparent for Event 3 (Fig. 3) when soils were wetter and rainfall was more intense.

By the end of Event 2c, the flush-out of evaporative salts must be complete as no mineral salts were observed on the riverbanks, resulting in lower concentrations than pre-Event 1 values. Similar trends have been observed in Contrary Creek, Virginia by Dagenhart (1980) and Boulder Creek, Iron Mountain, California by Keith et al. (2001).

During Event 1 pH decreased very slightly from 2.31 to 2.27 (Fig. 3), despite the increase in discharge. In comparison, the large influxes of freshwater in Event 2c (Q_{max} = 76.8 m^3/s) and Event 3 (Q_{max} = 127 m^3/s), when soluble salts are washed, increased pH to 3.56 and 3.36, respectively.

The mineralogy and chemistry of 15 salt mineral samples collected in August 2003 and September 2004 are summarised in Table 3. In addition to iron-rich salt minerals (copiapite, coquimbite, melanterite, rozenite and szomolnokite), XRD identified variable quantities of minerals containing Al (alunogen, aluminocopiapite and halotrichite), Ca (gypsum) and Mg (hexahydrite). Absolute and relative concentrations were highly variable (Table 3). Wide variations in mineralogy and chemistry have been noted before in salt minerals from the Río Tinto (Buckby et al., 2003; Lottermoser, 2005) and other mining regions (e.g. Keith et al., 2001).

Fe/SO_4 ratios were generally higher during the flood events than during the low-flow conditions of early October (Fig. 4). Efflorescent soluble salts have higher Fe/SO_4 ratios than river water (Fig. 5a), so their dissolution increases the Fe/SO_4 ratio. Variations in Fe/SO_4 ratios throughout the flood events can be explained by a mixing of freshwater with acidic leachates coming from the Riotinto Mining District (Fig. 5a). The dissolution of soluble salts might have a higher influence on water chemistry during the first events, decreasing its significance as these soluble salts are progressively washed. Furthermore, the precipitation

Table 2 Basic statistics of results obtained during the flood events

		n	Mean	Median	Standard deviation	Minimum	Maximum	Percentile		Peak 2b/ Peak 3	Detection limit
								25	75		
Flow	m^3/s	25	12.5	3.7	20.6	0.004	87.3	1.46	13.7		
pH		25	2.70	2.75	0.42	2.25	3.56	2.31	2.95		
EC	m S/cm	25	3.87	2.13	3.02	0.51	8.08	1.11	6.67		
Eh	mV	25	726	735	74	608	840	664	783		
Main elements (mg/L)	SO_4	25	3583	1272	3572	158	9474	443	6437	2.5	0.09
	Al	25	192	82	186	7.0	483	26	343	3.1	0.06
	Ca	25	86	43	69	13	184	24	151	0.6	0.06
	Cu	25	55	20	57	1.6	148	5	102	3.8	0.08
	Fe	25	489	133	522	10	1385	35	969	4.2	0.03
	K	25	2.7	1.9	2.1	0.6	8.5	1.3	3.2	0.03	0.06
	Mg	25	184	67	179	10	463	24	343	2.2	0.08
	Mn	25	25	12	21	2.1	56	5	47	1.2	0.07
	Na	25	28	16	22	6.2	64	8	49	0.4	0.08
	Si	25	25	15	22	3.9	69	5	39	0.6	0.02
	Zn	25	55	17	57	1.7	145	6	107	3.8	0.14
Trace elements (μg/L)	As	25	316	40	349	6	879	12	651	5.2	2.73
	Ba	24	40	35	23	13	104	24	46	0.02	0.20
	Be	20	10	12	8	1.3	23	3	17	1.4	1.10
	Cd	25	274	82	283	9	740	25	507	3.4	1.31
	Co	25	1618	602	1616	62	4142	191	3091	3.0	1.94
	Cr	25	60	15	64	1.3	181	3	113	4.9	1.75
	Li	25	320	276	291	13	803	41	568	2.5	1.55
	Mo	24	49	13	48	1.5	131	8	91	3.8	2.31
	Ni	25	493	226	493	23	1279	55	926	2.4	1.22
	P	24	550	518	499	28	1191	50	1021	1.8	7.04
	Pb	25	508	402	322	80	1637	313	619	0.01	2.20
	Sn	23	54	12	52	0.9	130	7	106	24	0.55
	Sr	25	219	138	153	39	483	84	334	0.04	0.07

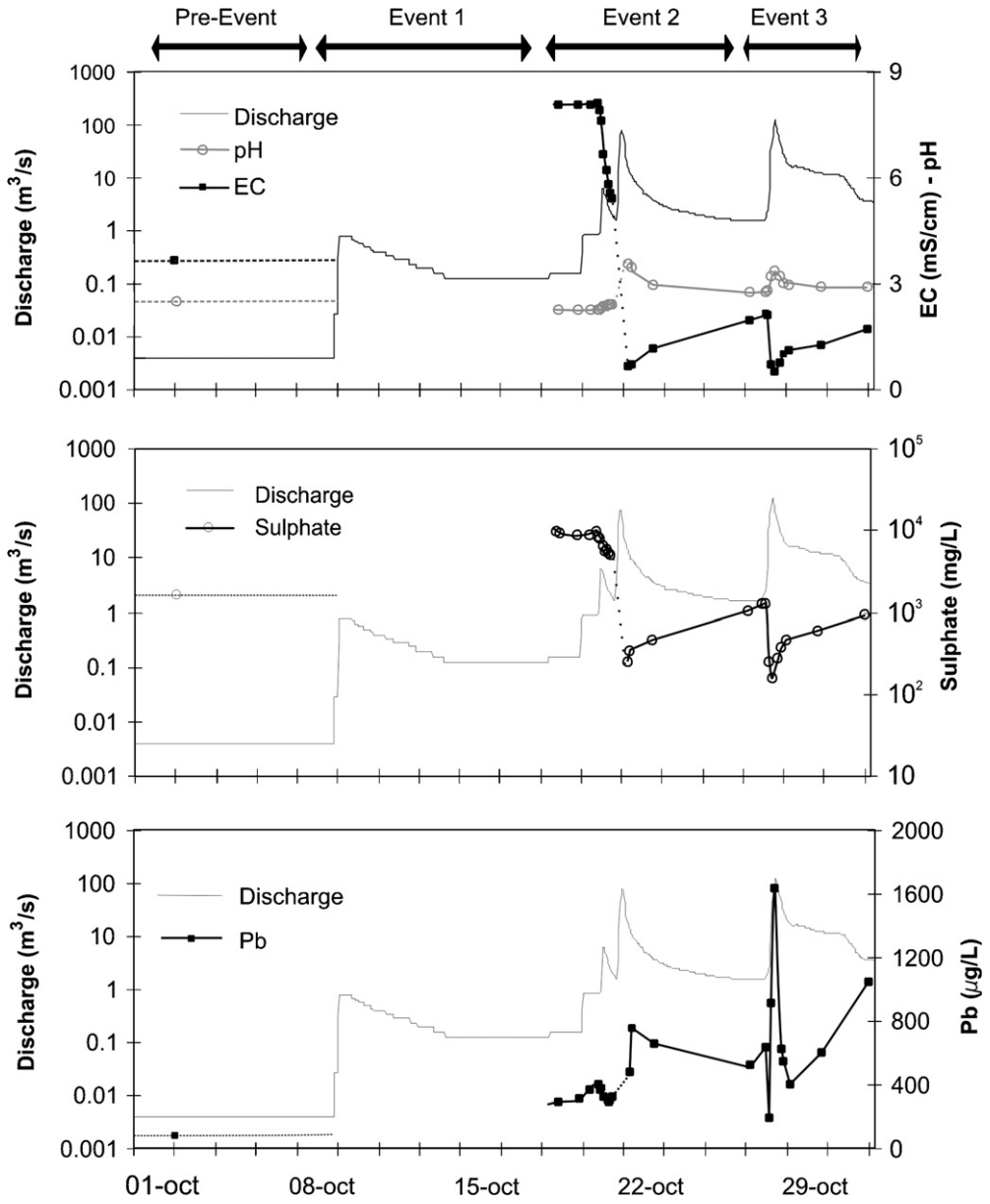

Figure 3 Variations in pH, electrical conductivity and sulphate and Pb dissolved concentrations.

of Fe oxyhydroxysulphates during the flood peaks 2c and 3 (samples with low Fe/SO_4 in Fig. 5a), when pH values were higher, also diminishes the Fe/SO_4 ratio.

Cu/Zn and Zn/ SO_4 ratios are also shown in Fig. 4. Cu and Zn should not sorb significantly to Fe oxyhydroxides at the low pH of the waters sampled in this study (Smith, 1999). Lee et al. (2002) investigated metal removal in the laboratory by neutralising 3 AMD stream waters from Tennessee, USA. They showed that the pH at which 50% of the metals were removed from solution ranged from 4.6 to 6.1 for Cu and 5.6 to 7.5 for Zn. It is therefore unlikely that the variations observed in these ratios (Fig. 4) were due to sorption/coprecipitation processes.

Alpers et al. (1994) showed that melanterite ($FeSO_4 \cdot 7H_2O$) preferentially removed Cu to Zn from solution meaning that it should have relatively high Cu/Zn ratios. The decrease in Cu/Zn seen in Event 2c (Fig. 4) should therefore, theoretically, not be due to dissolution of melanterite or its dehydration products (rozenite $FeSO_4 \cdot 4H_2O$ or szomolnokite $FeSO_4 \cdot H_2O$). Furthermore, Buckby et al. (2003) showed that copiapite (rather than melanterite-suite minerals) was the most abundant salt mineral in the Río Tinto.

The similarity of Event 1 Cu/Zn ratios to pre-Event 1 ratios (Fig. 4) suggests that the weighted average of salt mineral compositions dissolved by Event 1 had similar ratios to the weighted average of summer inputs from the mining area. Variations in these ratios throughout the flood events may well reflect changes in the dominant mine drainage sources into the river (Fig. 5b) rather than non-conservative behaviour. Fig. 5c shows that variations in Zn/SO_4 ratio in most of samples could be explained as a mixing of two end-members: unaffected freshwaters (end-member A represented by the water composition in the Corumbel

Table 3 Mineralogy and chemistry of salt minerals collected in August 2003 (CH68-CH75) and September 2004 (CH157-CH260)

Location		CH68	CH71	CH73	CH74	CH75	CH157	CH163	CH179	CH204	CH209	CH253	CH254	CH255	CH256	CH260
		7.2	7.2	8.2	8.2	8.2	79	21	0.2	7.2	7.2	8.2	8.2	8.2	8.2	7.2
Mineralogy		Cp, Ha, Hx, Gyp	Rz, Cp, Ha, Hx	Me, Pi, Gyp, Jt	Sz, Rh, Al	FeCp, AlCp		Hx, Ha, Cp, S	Cp, Cq, Al	Ha	Rz, AlCp, Gu, Gyp	Rz,Me, Cp, Cq, Gyp	AlCp, Cq	Sz, Al, Rh, Cq	Cq, Sz, Al	Qz, AlCp, Al,Cq,Ha
Fe	%	6.85	12.4	29.1	21.4	23.2	0.42	2.78	17.1	0.32	20.3	29.0	15.6	27.9	20.2	6.91
Mg	%	3.20	5.08	0.28	0.23	0.17	4.26	6.40	2.11	2.69	4.11	0.80	0.10	0.31	0.17	0.79
Al	%	3.63	2.57	0.52	2.40	1.00	3.47	2.67	2.45	4.60	0.31	1.14	0.61	1.07	3.89	2.59
Na	%	0.59	0.22	0.16	0.26	0.10	3.41	0.74	0.04	0.24	0.16	0.16	0.12	0.18	3.13	0.17
Mn	%	0.43	0.64	0.05	0.05	0.05	0.57	0.66	0.03	0.43	0.62	0.05	0.05	0.05	0.05	0.10
Ca	%	0.29	<0.009	0.11	0.01	<0.009	0.06	<0.009	<0.009	<0.009	0.19	0.09	<0.009	0.03	<0.009	0.04
Si	%	0.22	<0.005	<0.005	<0.005	<0.005	<0.005	<0.005	<0.005	<0.005	<0.005	<0.005	<0.005	<0.005	<0.005	12.9
Ti	%	0.01	<0.003	<0.003	0.01	<0.003	<0.003	0.01	<0.003	<0.003	<0.003	<0.003	0.01	<0.003	<0.003	0.09
P	%	0.013	<0.003	<0.003	0.013	0.004	0.004	0.004	<0.003	<0.003	<0.003	<0.003	0.004	<0.003	0.004	0.004
K	%	<0.01	<0.01	<0.01	<0.01	<0.01	<0.01	<0.01	<0.01	<0.01	<0.01	<0.01	<0.01	<0.01	<0.01	0.46
Zn	mg/kg	11,300	4900	5240	4750	5510	17,500	12,100	183	13,800	7060	5130	4080	5260	4700	4190
Cu	mg/kg	12,200	765	4590	3380	4350	4850	5790	173	11,800	257	5640	3720	5100	3980	3560
Co	mg/kg	375	236	102	78	86	419	325	181	374	333	113	72	100	68	73
Pb	mg/kg	32	15	118	25	11	bdl	13	10	41	256	55	10	39	31	1060
Ni	mg/kg	98	41	25	29	23	81	152	13	36	24	30	21	26	30	22
Zr	mg/kg	16	<5	13	27	12	20	12	6	18	13	20	46	25	20	151
Cr	mg/kg	<5	5	12	29	23	27	8	10	<5	8	12	34	22	27	11
V	mg/kg	<2	7	17	36	15	<2	15	7	<2	10	16	13	18	30	33
Y	mg/kg	17	6	<5	10	<5	27	23	8	19	<5	<5	<5	<5	<5	50
Sr	mg/kg	6	8	<5	<5	<5	<5	7	<5	<5	13	<5	<5	<5	<5	19
Rb	mg/kg	<5	<5	<5	<5	<5	10	<5	<5	<5	<5	<5	<5	<5	6	26

Al = alunogen, AlCp = aluminocopiapite, Cp = copiapite, Cq = coquimbite, FeCp = ferricopiapite, Gu = gunningite, Gyp = gypsum, Ha = halotrichite, Hx = hexahydrite, Jt = jarosite, Me = melanterite, Pi = pisanite, Qz = quartz, Rh = rhomboclase, Rz = rozenite, S = $NaAl(SO_4)_2 \cdot 12H_2O$ (syn), Sz = szomolnokite.
S = $NaAl(SO_4)_2 \cdot 12H_2O$ (syn), Sz = szomolnokite.
Location: distance downstream from source (km).

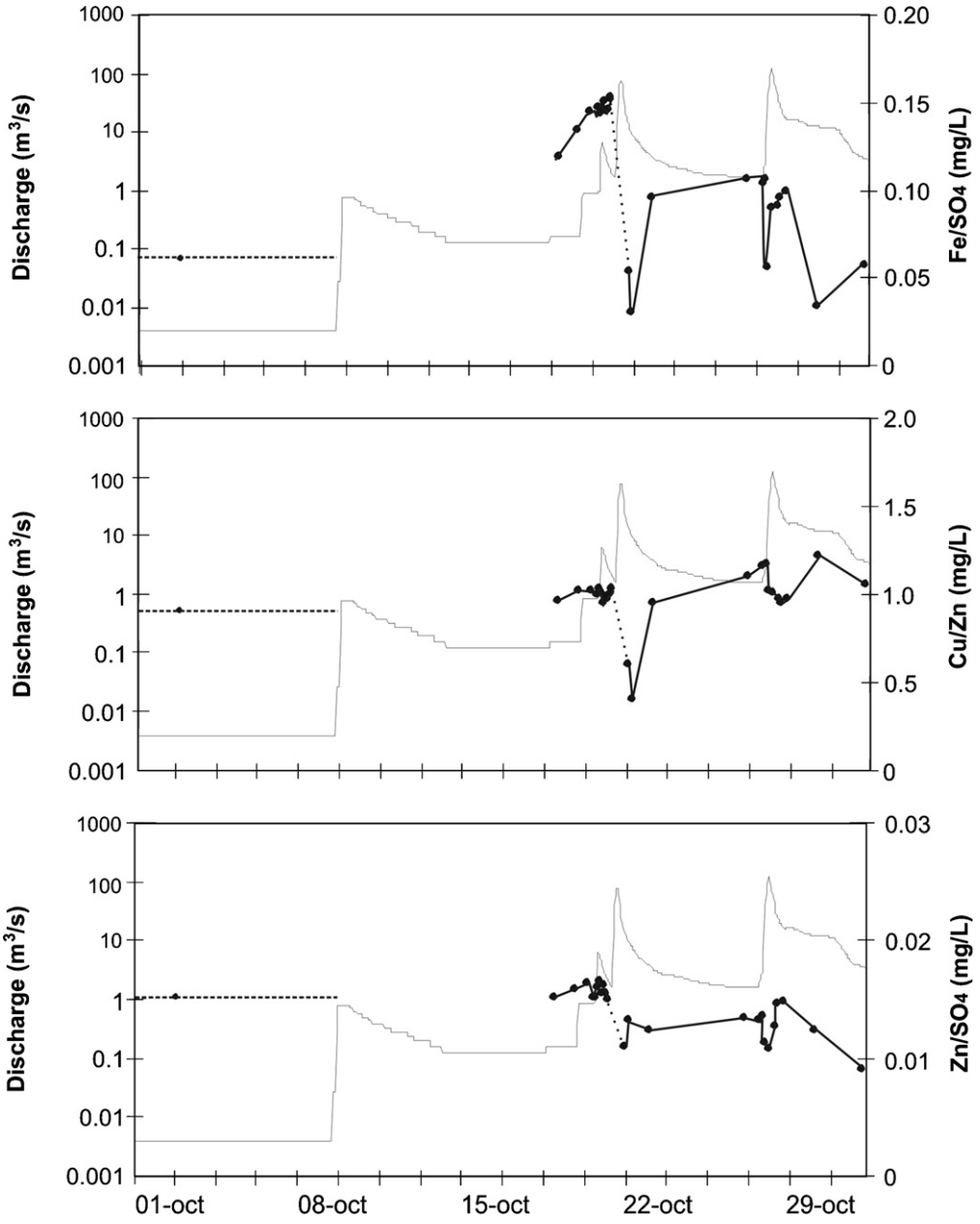

Figure 4 Variations in Fe/SO_4, Cu/Zn and Zn/SO_4 mass ratios.

reservoir) and Río Tinto water during event 2a (end-member B) as representative of maximum contamination level. Samples located away from this mixing line would indicate the influence of different AMD sources.

Saturation indices

To examine the phases controlling non-conservative behaviour, saturation indices (SIs) were calculated using the modelling program PHREEQC (Parkhurst and Appelo, 1999) and the WATEQ4F thermodynamic database (Ball and Nordstrom, 1991). The database was amended with solubility products for plumbojarosite ($Pb_{0.5}Fe_3(SO_4)_2(OH)_6$, $\log K_{sp} = -8.14$; Chapman et al., 1983) and schwertmannite ($Fe_8O_8(OH)_{4.5}(SO_4)_{1.75}$, $\log K_{sp} = 10.5$, Yu et al., 1999). Fe speciation was not analysed in the samples taken in October 2004 but modelling results (based on Eh) indicated an Fe(III) content of 81% prior to the flood events. The percentage of dissolved Fe(III) increased throughout the flush-out processes, reaching almost 99% of the total iron at the beginning of Event 2. These values agree with Fe speciation measured by Hubbard (2007) (Fe(III) = 81—98% of total Fe, $n = 5$). However, Fe(III) percentages gradually decreased as concentrations were diluted, reaching a minimum Fe(III) content of 3% of total iron (S20) during the third event. Geochemical modelling showed that all the sampled waters were oversaturated with respect to hematite (SI = 8.7—11.2) and goethite (SI = 3.3—4.6) although kinetic factors mean that these phases tend to form paragenetically from other metastable phases rather than precipitating directly

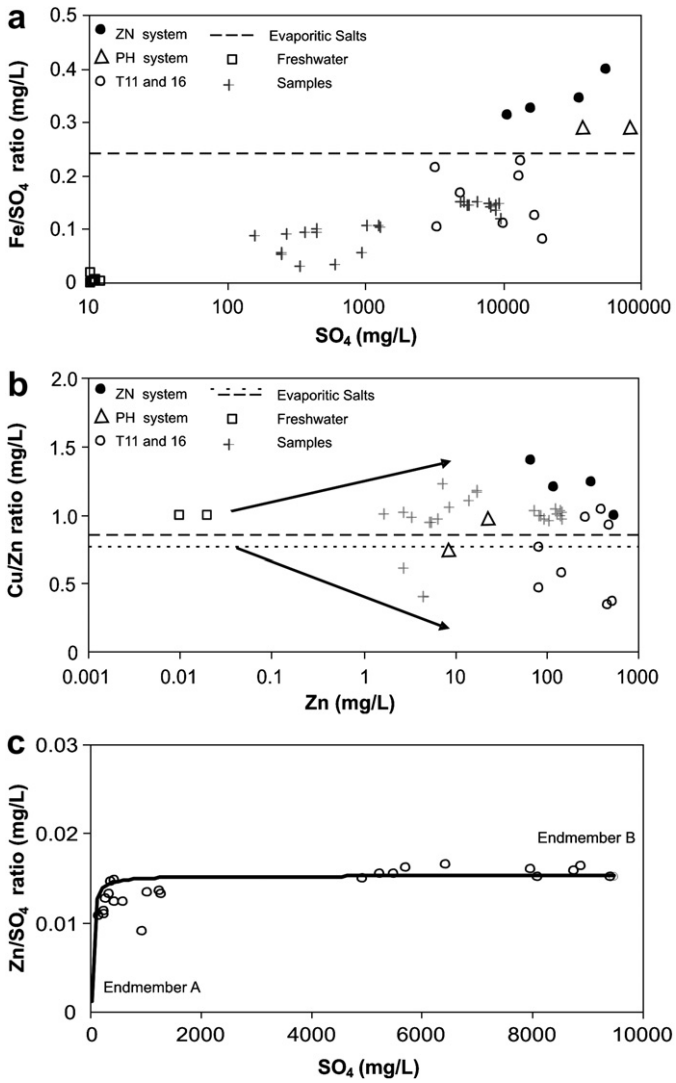

Figure 5 (a) Fe/SO_4 ratio *versus* SO_4 concentration; (b) Cu/Zn ratio *versus* SO_4 concentration; (c) Zn/SO_4 *versus* SO_4 concentration showing a mixing line between freshwater (end-member A) and the most contaminated sample (end-member B). Ionic ratio from evaporitic salts expressed as the median value from Buckby et al. (2003) (dashed line) and from this study (pointed line). AMD sources: Zarandas Naya System (ZN System), Tunnel 11 and 16 systems (T11 and T16) and Peña del Hierro system (PH system). Freshwater data are from the Corumbel reservoir.

from solution (Bigham et al., 1996; Nordstrom and Alpers, 1999). In terms of the metastable phases, the samples were generally undersaturated with amorphous $Fe(OH)_3$ (SI = −2.5 to −0.9), as would be expected in these low pH waters, and generally oversaturated with respect to schwertmannite (SI = −4.3 to 5.5) and K-jarosite (SI = −1.6 to 2.9).

The behaviour of Pb in Fig. 3 could not be explained from the modelling output by equilibrium with a solid phase as all samples were undersaturated with respect to anglesite ($PbSO_4$, SI $\leqslant$ −0.50) and (with the exception of sample S1) oversaturated with plumbojarosite (SI = −0.64 to 3.2). It is possible that a detailed examination of the suspended particulate matter carried by flood events may yield an explanation for Pb behaviour. All samples were oversaturated with respect to barite ($BaSO_4$, SI = 0.2−0.8) although Ba concentrations could potentially be explained by equilibrium with a mixed Ba-Sr sulphate phase as celestite ($SrSO_4$) was undersaturated in all samples (SI $\leqslant$ −1.3). Alternatively, barite oversaturation could potentially be explained by colloidal barite (<0.45 μm) in the samples (Naus et al., 2005). However, Ba is not an important contaminant in this system as sampled concentrations (13−104 μg/L) were all below World Health Organisation drinking water quality guidelines (0.7 mg/L; WHO, 2004).

Pollutant loads

Instantaneous pollutant loads (mass of pollutant transported per unit time, L_i) were calculated as the product of instantaneous discharge and concentration. Most elements showed a similar temporal evolution, as typified by Zn in Fig. 6. For Zn, loads increased from 0.099 g/s on 02/10/04 to 23 g/s at the end of Event 1. The highest instantaneous loads occurred in Event 2 reaching peaks of 130 g/s in Event 2a and 820 g/s in Event 2b. By the

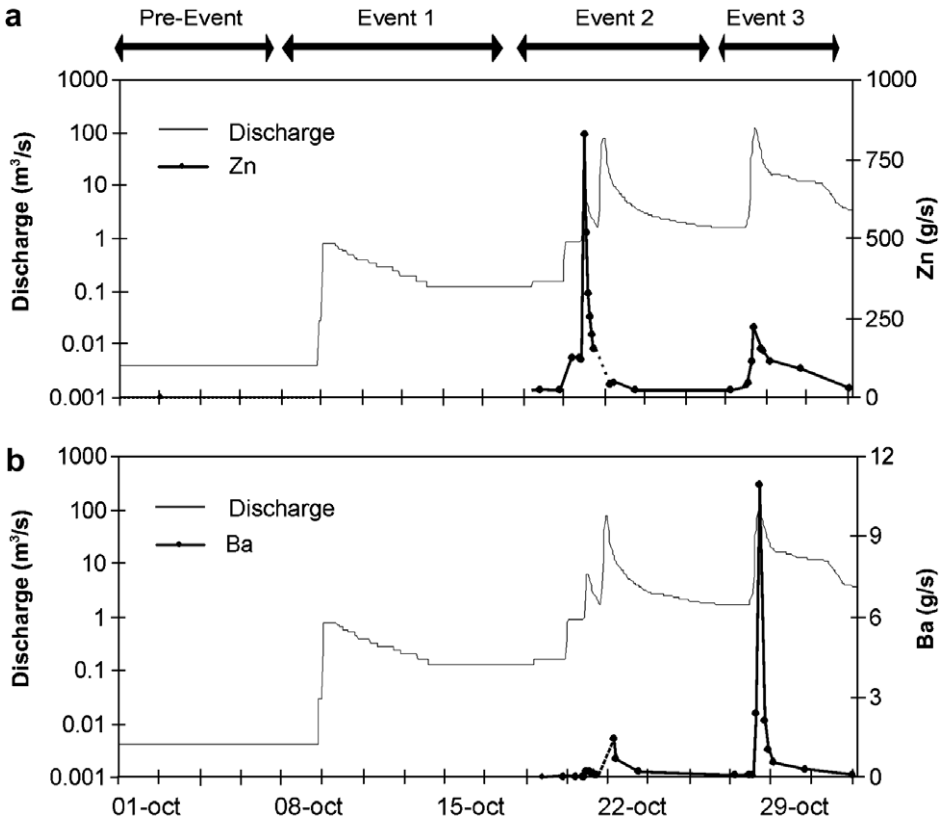

Figure 6 Instantaneous dissolved loads of Zn and Ba.

end of Event 2c, field observations indicated that all of the salt minerals on the riverbanks had been dissolved and L_i had decreased to 21 g/s. The less pronounced increase in L_i observed in Event 3 was therefore not due to salt mineral dissolution from the riverbanks. Possible explanations include the dissolution of any remaining salt minerals within spoil heaps, the expellation of pore fluids from spoil heaps and increased mineral leaching during Event 3.

Differences between elements can be summarised by a ratio comparing peak L_i values in Event 2b and Event 3 (Peak 2b/Peak 3). For most elements, this ratio varies between 1.2 and 5.2 (Table 2). Elements with a ratio below 1 include Ca, K, Na, Si and Sr, all of which are present in the freshwater tributaries as well as the mining inputs. As with concentration profiles, Pb and Ba behave differently (Fig. 6). The highest measured L_i for each element occurred at the peak of Event 3 although it is also possible that similar peaks in L_i occurred in Event 2c but no samples were taken.

Total pollutant load estimations for October 2004 were calculated by establishing relationships between discharge and dissolved concentrations (Olías et al., 2006). Examples are shown in Fig. 7. Three different time periods were selected with good correlations: (1) from 20th October at 17:00 to 21st at 01:00 (the falling limb of Event 2b), (2) from 21st at 18:00 to 27th at 11:00 (the falling limb of Event 2c) and (3) from 27th at 14:00 onwards (Event 3). Where significant correlations ($p < 0.01$) were not established or datasets were incomplete, the pollutant load for each element was estimated as follows:

(1) From 1st October (00:00) to 9th October (08:00): discharge (0.004 m^3/s) was multiplied by time and the concentration of sample S1.
(2) From 9th October (08:00) to 14th October (00:00): total discharge in the event was multiplied by the mean concentration of samples S1 and S2.
(3) From 14th October (00:00) to 18th October (19:00): total discharge was multiplied by the concentration of sample S2.
(4) From 18th October (19:00) to 20th October at 17:00, the following expression was applied:

$$L_T = \sum 1/2(C_{i(n)} + C_{i(n+1)})Q_{T(n\rightarrow n+1)}$$

where L_T = total load, C_i = instantaneous concentration for sample n, Q_T = total discharge.

Fig. 7 also highlights an interesting comparison between the falling limbs of Event 2c and Event 3. Even though Event 2c was earlier in the month (and therefore may be expected to have access to salt minerals and concentrated pore fluids), for many elements the falling limb of the event had lower concentrations for any given discharge than the falling limb of Event 3. This can be explained by the different rainfall distributions in each event. Fig. 8 shows that the rainfall maximum for Event 2c was located to the west of the mining area, leading to a large input of diluting freshwater during this event. In contrast, Event 3 was focused on the mining area itself. As mentioned before, the higher rainfall in Event 3 combined with earlier rainfall during the month meant that large inputs of freshwater from the

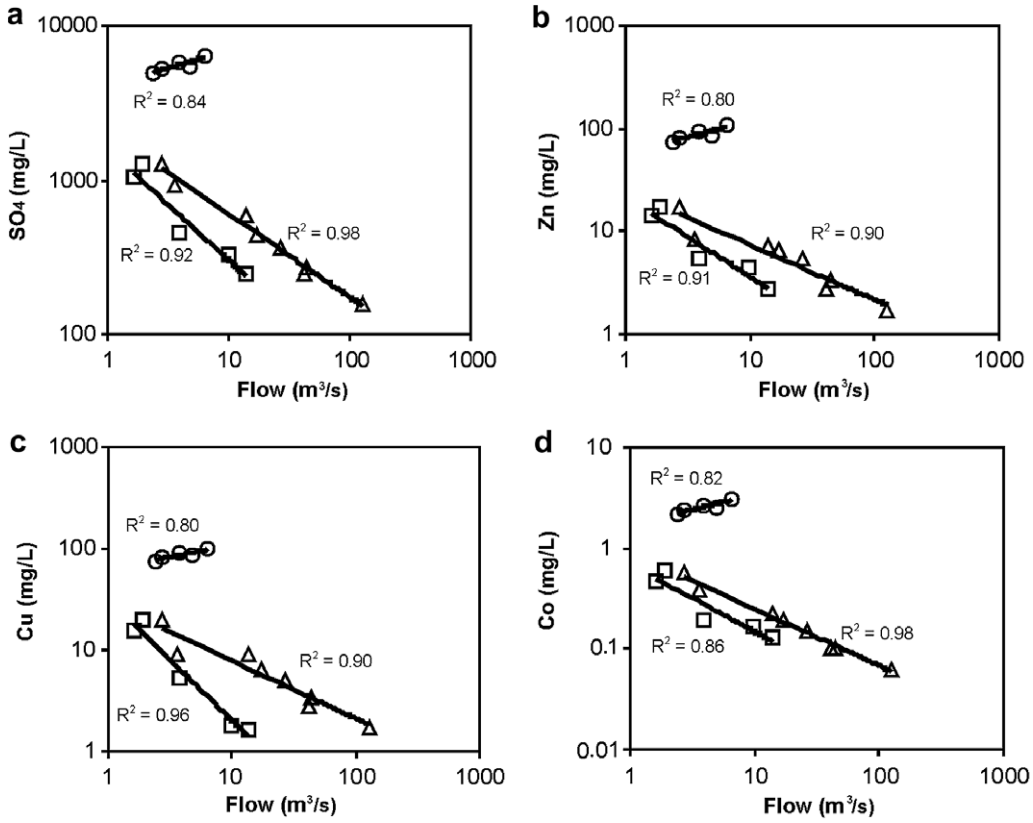

Figure 7 Examples of relationships between discharge and dissolved concentrations during October 2004 (circles = from 20th at 17:00 to 21st at 01:00; squares = from 21st at 18:00 to 27th at 11:00; and triangles = from 27th at 14:00 on).

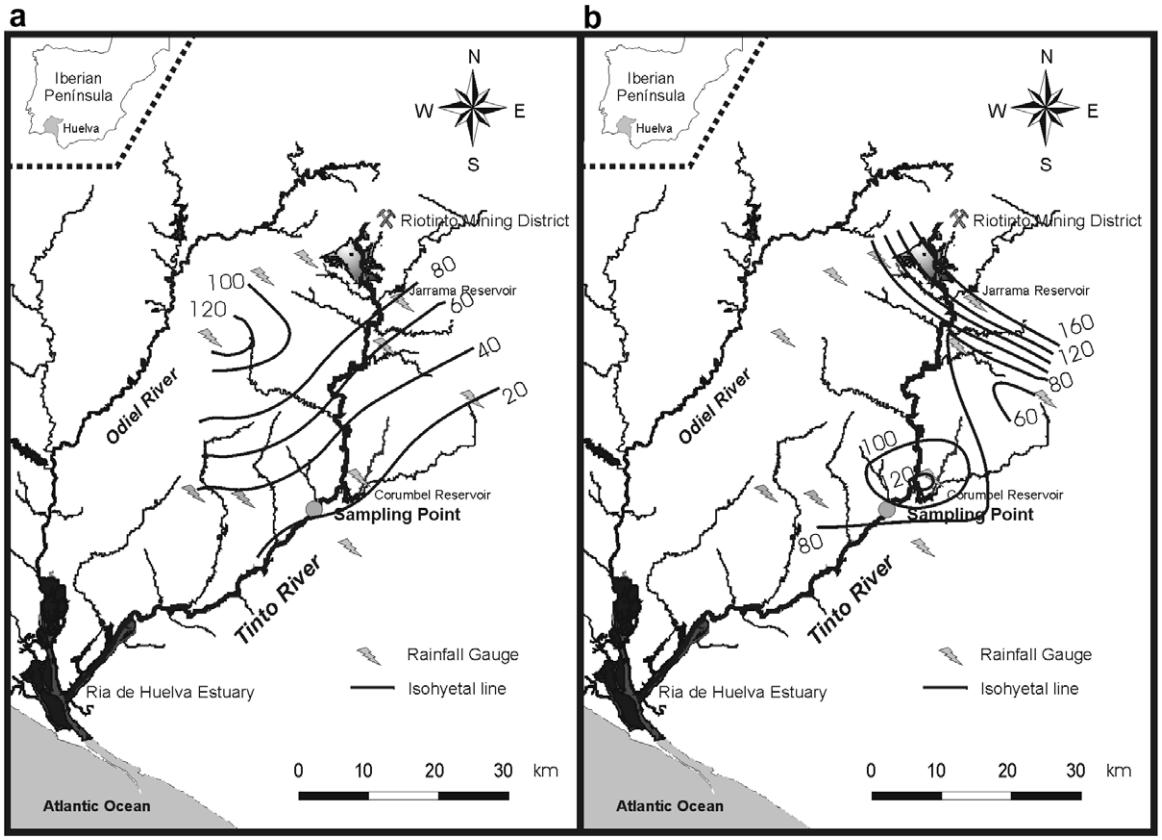

Figure 8 Rainfall distribution in the Río Tinto basin during: (a) Event 2; (b) Event 3.

Table 4 Pollutant load estimates for the Río Tinto (tonnes)

	Braungardt 1 Year	Sainz 1 Year	Olías 1 Year	This study September 2004	This study October 2004	This study as % of Olías
Al	–	–	1224	0.92	420	34
As	–	9.5	12.4	0.0001	0.41	3.3
Ba	–	–	–	0.0004	0.70	–
Cd	0.86	2.8	3.9	0.0013	0.49	13
Co	3.3	–	8.7	0.0071	3.3	38
Cr	–	1.4	–	0.0002	0.10	–
Cu	88	284	469	0.23	100	21
Fe	1540	–	5075	1.0	770	15
Li	–	–	–	0.0029	0.58	–
Mn	61	85	163	0.11	71	44
Ni	1.4	2.7	2.2	0.0023	1.0	45
Pb	0.87	1.8	14.8	0.0008	6.8	46
SO_4	–	–	36,589	17	5700	16
Zn	240	596	863	0.26	100	12

Braungardt et al. (2003), Sainz et al. (2004) and Olías et al. (2006).

Jarrama Reservoir did flow into the river but not until the latter stages of the event, causing the stepped profile of the falling limb (Fig. 2).

Table 4 compares the total loads estimated for October 2004 with September 2004 and with previous estimates of annual loads. The total load for September 2004 was calculated using sample S1 and a discharge of 0.004 m^3/s. This approach is justified as samples taken ~11 km further downstream in September 2004 and early October 2004 showed little variation during this time period (e.g. $SO_4 = 1320 \pm 69$ mg/L, mean $\pm 1\sigma$, $n = 6$). Overall the Río Tinto transported approximately 1000 times more water in October 2004 than September 2004 and between 140 (Na) and 8200 (Pb) times more dissolved elements, highlighting the extreme seasonality of water flow and pollutant transport in this river and the key role of flood events.

In October 2004, 330 to 530 times more metals (Al, Cd, Co, Cr, Cu, Mg, Ni, Zn) and sulphate than September 2004 were transported, with slightly higher values of Fe (770) and Mn (655). The elements mobilised to the greatest degree by the additional water provided by the storm events and tributaries were Pb (8200), As (5500), Ba (1900), Mo (1000) and K (880). If anything, these values underestimate the total loads transported because only limited data was available for Events 1 and 2c. During October 2004, Fe and Al were the dominant metals transported by the Río Tinto followed by Cu, Zn and Mn with lesser quantities of toxic trace elements such as Pb, Co, Ni, Li, Cd, As and Cr.

In this study, salt minerals were observed to have been dissolved by the end of Event 2. Events 1 and 2 combined transported approximately 58 t of Zn and 55 t of Cu. These estimates represent a possible upper limit for the amount of Zn and Cu stored by salt minerals in summer 2004, although as previously mentioned, neither Event 1 nor Event 2c were sampled in detail. In comparison, Buckby et al. (2003) extrapolated salt mineral coverage, density, porosity and chemical composition data to be 200 t of Zn and 150 t of Cu stored as salt minerals during the summer and dissolved by the first rainfall events of the autumn. The estimates by Buckby et al. (2003) and this study compare well, allowing for differences in the methodology used.

Extrapolating the data from September 2004 and October 2004 to create a yearly total is unwise given the inter- and intra-monthly variations in loads. Nevertheless, some comparisons can be made with previous estimations of annual metal loads (Table 4). Note the differences in the

Table 5 Comparison of flood events in different AMD catchments

	Río Tinto	Boulder Creek	Contrary Creek
	This study	Keith et al. (2001)	Dagenhart (1980)
Q_{max} (m^3/s)	127	17	0.58
pH	2.3 – 3.6	3.0	2.9 – 4.0
Fe_{max} (mg/L)	1390	94	230
Al_{max} (mg/L)	483	63	–
Zn_{max} (mg/L)	145	5.5	70
Cu_{max} (mg/L)	148	3.7	17
Fe_{max} (g/s)	7500	47	69
Al_{max} (g/s)	2700	31	–
Zn_{max} (g/s)	820	2.7	21
Cu_{max} (g/s)	830	1.8	3.7

annual estimates. This is due to differences in both the years studied and the frequency of samples. Braungardt et al. (2003) extrapolated annual loads based on only 4 samples from different seasons in 1996–1998. The estimates for Sainz et al. (2004) were calculated in this study from their mean hourly loads (1988–2001). Sampling frequency was not given but appears to be quarterly. Finally, the estimates by Olías et al. (2006) were based on 419 samples collected between 1995 and 2003 (52 samples on average per year) and therefore are likely to be the most accurate published estimates.

Comparing the results of this study with Olías et al. (2006), it is striking that in October 2004 alone, almost 50% of the annual loads of Pb, Mn and Ni were transported to the Ría of Huelva estuary, once again highlighting the importance of flood events. At the other extreme, the As loads transported in October 2004 correspond to only 3% of the annual total although Olías et al. (2006) did note that their As and Pb estimations had the highest uncertainties. These two elements showed the greatest difference between low-flow and flood regimes in this study.

Comparison with other AMD sites

Several studies have investigated the hydrochemical responses of small catchments affected by AMD (Gammons et al., 2005; Lambing et al., 1999; Sandén et al., 1997; Wirt et al., 1999) while the temporary storage of metals by salt mineral formation in dry periods followed by dissolution and metal release by rainfall/flood events has been studied or proposed as an important physicochemical process in a number of other works (Alpers et al., 1994; Bayless and Olyphant, 1993; Cravotta, 1994; Dagenhart, 1980; Hammarstrom et al., 2005; Keith et al., 2001).

Table 5 compares the characteristics of flood events in this study with Contrary Creek, Virginia (Dagenhart, 1980) and Boulder Creek, Iron Mountain, California (Keith et al., 2001). Instantaneous metal loads were calculated from discharge-time and concentration-time graphs. Both of these studies displayed peaks in concentration associated with initial increases in discharge followed by decreases in concentration as discharge continued to rise. It is clear from these results that the Río Tinto represents the most extreme example of salt mineral dissolution studied to date with the highest metal concentrations and loadings. Previous studies on the adjacent Odiel River have calculated that it transports a higher dissolved load as it drains a considerably larger catchment containing many mines. However, concentrations are much lower and the pH is higher. Ongoing work at the University of Huelva is examining flood events in this river using high-resolution temporal sampling.

In terms of the environmental impact on the estuary, elevated loads are arguably more important than elevated concentrations in the Río Tinto, because concentrations are rapidly diluted and pH increased as the Río Tinto water mixes with seawater and salinity increases in the estuary (Braungardt et al., 2003). Higher loads may therefore cause elevated concentrations to persist further into the estuary. Large, high-velocity discharges are also important because they mobilise the highest amount of sediment, releasing metal-rich interstitial waters and increasing concentrations still further in the upper Río Tinto Estuary (Braungardt et al., 2003). The key role of these events in the pollutant transport in arid and semi-arid environments should be considered in all management strategies; these extreme variations in discharge and concentrations complicate the design of effective treatment schemes in such climates.

Conclusions

This work is the first detailed investigation of the hydrochemical variations in the Río Tinto during rainfall/flood events following a long dry season and it is likely the largest recorded example of a flush-out event in areas affected by AMD. Previous studies on the adjacent Odiel River show a higher yearly dissolved load transported by this river. Ongoing work is examining flood events and its impact on the metal load into the estuary.

As with previous studies examining rainfall events in AMD catchments (e.g. Dagenhart, 1980; Keith et al., 2001), dissolved concentrations increased dramatically following the first rainfall event of the season and then showed a general decrease throughout the month as the summer store of soluble evaporitic salt minerals and concentrated pore waters was progressively depleted and freshwater dilution processes became increasingly dominant.

Three separate rainfall/flood events were identified in the month. In general, concentrations peaked following the first event (Q_{max} = 0.78 m^3/s) while dissolved loads peaked in the second event (Q_{max} = 77 m^3/s) and discharge in the third event (Q_{max} = 127 m^3/s). Variations in relative concentrations were attributed to oxyhydroxysulphate precipitation, to relative changes in the sources of AMD (e.g. salt minerals, mine tunnels, spoil heaps etc.) and to a higher contribution of freshwaters as the flood events progressed.

Ba and Pb behaved anomalously with concentrations and loads peaking at different times to other elements. Ba behaviour could potentially be explained by equilibrium with a Ba–Sr sulphate or by colloidal barite but there was no clear explanation for Pb.

Although significant ($p < 0.01$) relationships existed between discharge and concentrations for certain periods, they could not be successfully extrapolated over the whole month or sometimes over a whole event. This highlights the need for high-resolution temporal sampling of these events in order to accurately estimate the annual dissolved load.

The dissolved pollutant load carried by the river during these floods was enormous. During October 2004, some 5700 t of sulphates, 770 t of Fe, 420 t of Al, 100 t of Cu, 100 t of Zn and 71 t of Mn were transported by the Río Tinto into the Ría of Huelva estuary. Approximately 1000 times more water and 140–8200 times more dissolved elements were transported in October 2004 compared with the low-flow regime of September 2004. Total loads in October 2004 correspond to 3% (As) to 46% (Pb) of the annual loads estimated by Olías et al. (2006) although more accurate annual loads (in dry and wet years) involving detailed sampling of flood events are needed to properly assess the contribution of flood events.

Acknowledgements

The authors wish to thank the Guadiana Hydrographic Confederation, and the Environmental Council of the Andalusia Regional Government for the information provided for this study, which has been financed through the project ''Mining contamination evaluation, acid mine drainage treatment, hydrologic modelling of the Odiel River basin and study of the contaminant load to the Huelva estuary'', financed by the Environmental Council of the Andalusia Regional Government, and CTM2006-28148-E/TECNO — CTM2007-66724-C02-02/TECNO financed by the Spanish Ministry of Education and Science. Chris Hubbard was funded by a University of Reading Postgraduate Studentship.

References

Acero, P., Ayora, C., Torrentó, C., Nieto, J.M., 2006. The behaviour of trace elements during schwertmannite precipitation and subsequent transformation into goethite and jarosite. Geochimica et Cosmochimica Acta 70, 4130—4139.

Achterberg, E.P., Herzl, V.M.C., Braungardt, C.B., Millward, C.E., 2003. Metal behaviour in an estuary polluted by acid mine drainage: the role of particulate matter. Environmental Pollution 121, 283—292.

Alpers, C.N., Nordstrom, D.K., Thompson, J.M., 1994. Seasonal variations of Zn/Cu ratios in acid-mine water from Iron-Mountain, California. In: Alpers, C.N., Blowes, D.W. (Eds.), Environmental Geochemistry of Sulfide Oxidation, ACS Symposium Series 550, pp. 324—344.

Ball, J.W., Nordstrom, D.K., 1991. WATEQ4F — User's manual with revised thermodynamic data base and test cases for calculating speciation of major, trace and redox elements in natural waters, U.S. Geological Survey Open-File Report 90—129, 185p.

Bayless, E.R., Olyphant, G.A., 1993. Acid-generating salts and their relationship to the chemistry of groundwater and storm runoff at an abandoned mine site in Southwestern Indiana, USA. Journal of Contaminant Hydrology 12, 313—328.

Bigham, J.M., Schwertmann, U., Traina, S.J., Winland, R.L., Wolf, M., 1996. Schwermannite and the chemical modeling of iron in acid sulfate waters. Geochimica et Cosmochimica Acta 60, 2111—2121.

Boyle, E.A., Huested, S.S., Grant, B., 1982. The chemical mass-balance of the Amazon plume: II, copper, niquel and cadmium. Deep Sea Research 29, 1355—1364.

Boyle, E.A., Chapnick, S.D., Bai, X.X., Spivack, A., 1985. Trace-metal enrichments in the Mediterranean Sea. Earth and Planetary Science Letters 74, 405—419.

Braungardt, C.B., Achterberg, E.P., Elbaz-Poulichet, F., Morley, N.H., 2003. Metal geochemistry in a mine polluted estuarine system in Spain. Applied Geochemistry 18, 1757—1771.

Buckby, T., Black, S., Coleman, M.L., Hodson, M.E., 2003. Fe-sulphate rich evaporative mineral precipitates from the río Tinto, Southwest Spain. Mineralogical Magazine 67 (2), 263—278.

Cánovas, C.R., Olias, M., Nieto, J.M., Sarmiento, A.M., Cerón, J.C., 2007. Hydrogeochemical characteristics of the Odiel and Tinto rivers (SW Spain). Factors controlling metal contents. Science of the Total Environment 373, 363—382.

Chapman, B.M., Jones, D.R., Jung, R.E., 1983. Processes controlling metal ion attenuation in acid mine drainage streams. Geochimica et Cosmochimica Acta 47, 1957—1973.

Cravotta, C.A., 1994. Secondary iron-sulfate minerals as sources of sulphate and acidity — geochemical evolution of acidic groundwater at a reclaimed surface coal-mine in Pennsylvania. In: Alpers, C.N., Blowes, D.W. (Eds.), Environmental Geochemistry of Sulfide Oxidation, ACS Symposium Series 550, pp. 345—364.

Dagenhart Jr., T.V., 1980. The acid mine drainage of Contrary Creek, Louisa County, Virginia: factors causing variations in stream water chemistry. M.Sc., thesis, Univ. Virginia, Charlottesville, Virginia.

Drever, J.I., 1997. The Geochemistry of Natural Waters: Surface and Groundwater Environments. Prentice Hall, New Jersey, 437p.

Elbaz-Poulichet, F., Morley, N.H., Cruzado, A., Velasquez, Z., Achterberg, E.P., Braungardt, C.B., 1999. Trace metal and nutrient distribution in an extremely low pH (2.5) river-estuarine system, the Ria of Huelva (South-West Spain). Science of the Total Environment 227, 73—83.

Elbaz-Poulichet, F., Braungardt, C., Achterberg, E., Morley, N., Cossa, D., Beckers, J., Nomérange, P., Cruzado, A., Leblanc, M., 2001. Metal biogeochemistry in the Tinto-Odiel rivers (Southern Spain) and in the Gulf of Cadiz: a synthesis of the results of the TOROS project. Continental Shelf Research 21, 1961—1973.

Elbaz-Poulichet, F., Seidel, J.L., Casiot, C., Velasquez, Z., Tusseau-Vuillemin, M.H., 2006. Short-term variability of dissolved trace element concentrations in the Marne and Seine Rivers near Paris. Science of the Total Environment 367, 278—287.

Fernández-Remolar, D., Rodriguez, N., Gómez, F., Amils, R., 2003. Geological record of an acidic environment driven by iron hydrochemistry: the Tinto River system. Journal of Geophysical Research 108 (E7) (Art. No. 5080).

Fernández-Remolar, D., Gómez-Elvira, J., Gómez, F., Sebastián, J., Martín, J., Manfredi, J.A., Torres, J., González Kessler, C., Amils, R., 2004. The Tinto river, an extreme acidic environment under control of iron, as an analog of the Terra Meridiani hematite site of Mars. Planetary and Space Science 52, 239—248.

Fernández-Remolar, D., Morris, R.V., Gruener, J.E., Amils, R., Knoll, A.H., 2005. The Río Tinto Basin, Spain: Mineralogy, sedimentary geobiology, and implications for interpretation of outcrop rocks at Meridiani Planum, Mars. Earth and Planetary Science Letters 240, 149—167.

Ferris, F.G., Hallbeck, L., Kennedy, C.B., Pedersen, K., 2004. Geochemistry of acidic Rio Tinto headwaters and role of bacteria in solid phase metal partitioning. Chemical Geology 212, 291—300.

Galán, E., Gómez-Ariza, J.L., González, I., Fernández-Caliani, J.C., Morales, E., Giráldez, I., 2003. Heavy metal partitioning in river sediments severely polluted by acid mine drainage in the Iberian Pyrite Belt. Applied Geochemistry 18, 409—421.

Gammons, C.H., Shope, C.L., Duaime, T.E., 2005. A 24 h investigation of the hydrogeochemistry of baseflow and stormwater in an urban area impacted by mining: Butte, Montana. Hydrological Processes 19, 2737—2753.

González-Toril, E., Llobet-Brossa, E., Casamajor, E.O., Amann, R., Amils, R., 2003a. Microbial ecology of an extreme acidic environment, the Tinto River. Applied and Environmental Microbiology 69, 4853—4865.

González-Toril, E., Gómez, F., Rodríguez, N., Fernández Remolar, D., Zuluaga, J., Marín, I., Amils, R., 2003b. Geomicrobiology of the Tinto River, a model of interest for biohydrometallurgy. Hydrometallurgy 71, 301—309.

Hammarstrom, J.M., Seal, R.R., Meier, A.L., Kornfeld, J.M., 2005. Secondary sulfate minerals associated with acid drainage in the eastern US: recycling of metals and acidity in surficial environments. Chemical Geology 215, 407—431.

Hubbard, C.G., 2007. Acid mine drainage generation and transport processes in the Tinto River, SW Spain, Ph.D., thesis, University of Reading, UK.

Hudson-Edwards, K.A., Schell, C., Macklin, M.G., 1999. Mineralogy and geochemistry of alluvium contaminated by metal mining in the Rio Tinto area, Southwest Spain. Applied Geochemistry 14, 1015—1030.

Keith, D.C., Runnells, D.D., Exposito, K.J., Chermak, J.A., Levy, D.B., Hannula, S.R., Watts, M., Hall, L., 2001. Geochemical models of the impact of acidic groundwater and evaporative sulphate salts on Boulder Creek at Iron Mountain, California. Applied Geochemistry 16, 947–961.

Lambing, J.H., Nimick, D.A., Cleasby, T.E., 1999. Short-term variation of trace-element concentrations during base flow and rainfall runoff in small basins, U.S. Geological Survey, Open-File Report 99–159, 32p.

Leblanc, M., Morales, J.A., Borrego, J., Elbaz-Poulichet, F., 2000. 4.500 year old mining pollution in Southwestern Spain: long-term implications for modern mining pollution. Economical Geology 95, 655–662.

Lee, J.H., Bang, K.W., 2000. Characterization of urban stormwater runoff. Water Research 34, 1773–1780.

Lee, G., Bigham, J.M., Faure, G., 2002. Removal of trace metals by coprecipitation with Fe, Al and Mn from natural waters contaminated with acid mine drainage in the Ducktown Mining District, Tennessee. Applied Geochemistry 17, 569–581.

López-Archilla, A.I., Marin, I., Amils, R., 2001. Microbial community composition and ecology of an acidic aquatic environment: the Tinto River, Spain. Microbial Ecology 41, 20–35.

López-Archilla, A.I., Gérard, E., Moreira, D., López-García, P., 2004. Macrofilamentous microbial communities in the metal rich and acidic river Tinto, Spain. FEMS Microbiology Letters 235, 221–228.

López-González, N., Borrego, J., Morales, J.A., Carro, B., Lozano-Soria, O., 2006. Metal fractionation in oxic sediments of an estuary affected by acid mine drainage (South-western Spain). Estuarine, Coastal and Shelf Science 68, 297–304.

Lottermoser, B.G., 2005. Evaporative mineral precipitates from a historical smelting slag dump, Río Tinto, Spain. Neues Jahrbuch für Mineralogie – Abhandlungen (181/2), 183–190.

Malki, M., González-Toril, E., Sanz, J.L., Gómez, F., Rodríguez, N., Amils, R., 2006. Importance of the iron cycle in biohydrometallurgy. Hydrometallurgy 83, 223–228.

Naus, C.A., McCleskey, R.B., Nordstrom, D.K., Donohoe, L.C., Hunt, A.G., Paillet, F.L., Morin, R.H., Verplanck, P.L., 2005. Questa Baseline and Pre-Mining Ground-Water-Quality Investigation 5. Well Installation, Water-Level Data, and Surface- and Ground-Water Geochemistry in the Straight Creek Drainage Basin, Red River Valley, New Mexico, 2001–03, U.S. Geological Survey Scientific Investigations Report 2005–5088, 220p.

Neal, C., Jarvie, H.P., Whitton, B.A., Gemmell, J., 2000. The water chemistry of the River Wear, North-east England. Science of the Total Environment (251/252), 153–172.

Nieto, J.M., Sarmiento, A.M., Olias, M., Cánovas, C.R., Riba, I., Kalman, J., Delvalls, T.A., 2007. Acid mine drainage pollution in the Odiel and Tinto rivers (Iberian Pyrite Belt, SW Spain) and bioavailability of the transported metals to the Huelva estuary. Environment International 33, 445–455.

Nocete, F., Alex, E., Nieto, J.M., Sáez, R., Bayona, M.R., 2005. An archaelogical approach to regional environmental pollution in the South-western Iberian Peninsula related to Third Millenium B.C mining and metallurgy. Journal of Archaelogical Science 32, 1566–1576.

Nordstrom, D.K., Alpers, C.N., 1999. Geochemistry of acid mine waters. In: Plumlee, G.S., Logson, M.J. (Eds.), The Environmental Geochemistry of Mineral Deposits, Rev. Econ. Geol. 6A, pp. 133–160.

Olías, M., Cánovas, C.R., Nieto, J.M., Sarmiento, A.M., 2006. Evaluation of the dissolved contaminant load transported by the Tinto and Odiel rivers (South West Spain). Applied Geochemistry 21, 1733–1749.

Parkhurst, D.L., Appelo, C.A.J., 1999. User's guide to PHREEQC (Version 2) – A computer program for speciation, batch reaction, one-dimensional transport, and inverse geochemical calculations, USGS Water-Resources Investigations Report 99-4259, Denver, USA, 312p.

Ruiz, F., González-Regalado, M.L., Borrego, J., Morales, J.A., Pendón, J.G., Muñoz, J.M., 1998. Stratigraphic sequence, elemental concentrations and heavy metal pollution in Holocene sediments from the Tinto-Odiel Estuary, Southwestern Spain. Environmental Geology 34 (4), 270–278.

Ruiz, M.J., Carrasco, R., Pérez, R., Sarmiento, A.M., Nieto, J.M., 2003. Optimización del análisis de elementos mayores y traza mediante UN-ICP-OES en muestras de drenaje ácido de mina. Proceedings IV Iberian Geochemical Meeting, 14–18 Julio, Coimbra, Portugal, Universidad de Coimbra, pp. 402–404.

Sainz, A., Grande, J.A., De La Torre, M.L., 2004. Characterisation of heavy metal discharge into the Ria of Huelva. Environment International 30, 557–566.

Sandén, P., Karlsson, S., Düker, A., Ledin, A., Lundman, L., 1997. Variations in hydrochemistry, trace metal concentration and transport during a rain storm event in a small catchment. Journal of Geochemical Exploration 58, 144–155.

Sarmiento, A.M., Nieto, J.M., Olías, M., 2004. The contaminant load transported by the river Odiel to the Gulf of Cádiz (SW Spain). Applied Earth Science: IMM Transactions section B 113, 117–122.

Smith, K.S., 1999. Metal sorption on mineral surfaces: an overview with examples relating to mineral deposits. In: Plumlee, G.S., Logson, M.J. (Eds.), The Environmental Geochemistry of Mineral Deposits, Rev. Econ. Geol., 6A, pp. 161–182.

Stumm, W., Morgan, J., 1996. Aquatic Chemistry: Chemical Equilibria and Rates in Natural Waters. John Willey and Sons, New York, 1022p.

Thevenot, D.R., Moilleron, D., Lestel, L., Gromaire, M.C., Rocher, V., Cambier, P., Bonte, P., Colin, J.L., de Ponteves, C., Meybeck, M., 2007. Critical budget of metal sources and pathways in the Seine River basin (1994–2003) for Cd, Cr, Cu, Hg, Ni, Pb and Zn. Science of the Total Environment 375, 180–203.

Tornos, F., 2006. Environment of formation and styles of volcanogenic massive sulfides: the Iberian Pyrite belt. Ore Geology Reviews 28, 259–307.

van Geen, A., Boyle, E.A., Moore, W.S., 1991. Trace-metal enrichments in waters of the Gulf of Cadiz, Spain. Geochimica et Cosmochimica Acta 55, 2173–2191.

van Geen, A., Adkins, J.F., Boyle, E.A., Palanques, A., 1997. A 120 year record of widespread contamination from mining of the Iberian Pyrite Belt. Geology 25, 291–294.

Vink, R., Behrendt, H., Salomons, W., 1999. Development of the heavy metal pollution trends in several European rivers: an analysis of point and diffuse sources. Water Science and Technology 39, 215–223.

Walling, D.E., Foster, D.E., 1975. Variations in the natural chemical concentration of river water during flood flows, and the lag effect: some further comments. Journal of Hydrology 26, 237–244.

World Health Organisation (WHO), 2004. Guidelines for Drinking-Water Quality, third ed., Geneva.

Wirt, L., Leib, K.J., Bove, D.J., Mast, M.A., Evans, J.B., Meeker, G.P., 1999. Determination of Chemical-Constituent Loads During Base-Flow and Storm-Runoff Conditions Near Historical Mines in Prospect Gulch, Upper Animas River Watershed, Southwestern Colorado, U.S. Geological Survey, Open File Report 99-159.

Yu, J.Y., Heo, B., Choi, I.K., Cho, J.P., Chang, H.W., 1999. Apparent solubilities of schwertmannite and ferrydrite in natural stream waters polluted by mine drainage. Geochimica et Cosmochimica Acta 63, 3407–3416.

Zänker, H., Moll, H., Richter, W., Brendler, W., Hennig, C., Reich, T., Kluge, A., Hüttig, G., 2002. The colloid chemistry of acid rock drainage solution from an abandoned Zn–Pb–Ag mine. Applied Geochemistry 17, 633–648.

Zettler, L.A.A., Gomez, F., Zettler, E., Keenan, B.G., Amils, R., Sogin, M.L., 2002. Eukaryotic diversity in Spain's river of fire. Nature 417, 137.